Measurement and analysis of the strength differential effect of 6000-series aluminum alloy sheet

AKIYAMA Kaisei[1,a] * and KUWABARA Toshihiko[2,b]

[1]Department of Mechanical Systems Engineering, Graduate School of Engineering, Tokyo University of Agriculture and Technology, 2-24-16 Naka-cho, Koganei-shi, Tokyo 184-8588, Japan

[2]Division of Advanced Mechanical Systems Engineering, Institute of Engineering, Tokyo University of Agriculture and Technology, 2-24-16 Naka-cho, Koganei-shi, Tokyo 184-8588, Japan

[a]ks-akiyama@st.go.tuat.ac.jp, [b]kuwabara@cc.tuat.ac.jp

Abstract. The tension-compression asymmetry (TCA, referred to as the strength differential effect, SDE, for annealed materials) of a 1.1-mm-thick 6000-series aluminum alloy sheet, A6116-T4, which is 3-months age hardened is measured using a uniaxial tensile test and an in-plane compression test. It is found that the in-plane compressive flow stress is 1-7 % higher than the uniaxial tensile flow stress; therefore, the material exhibits the SDE. Moreover, a stacked compression test in the normal (through-thickness) direction (ND) of the test sample is also performed to measure the hydrostatic stress dependence of the yield stress. It is found that the uniaxial compressive flow stress in the ND is 4-9 % higher than the equibiaxial tensile flow stress measured using a cruciform equibiaxial tension test (ISO 16842); therefore, the hydrostatic stress dependence of the yield stress is confirmed. Hence, it is concluded that the SDE observed in A6116-T4 is caused by the hydrostatic stress dependence of the yield stress.

Introduction

Aluminum alloy sheets are used for manufacturing automotive parts to reduce the weight of car bodies. Automotive parts are mainly fabricated using press forming, which has superior productivity. During press forming, materials are subjected to compressive stress as well as tensile stress. Some metals have different work-hardening behavior in tension and compression, a phenomenon called the Tension-Compression Asymmetry (TCA). In particular, the TCA observed for the materials having no prestraining is referred to as the Strength Differential Effect (SDE).

The SDE in aluminum alloys has been previously investigated. Spitzig and Richmond [1] performed uniaxial tension and compression tests under hydrostatic pressure on both iron-based materials, including Fe single crystals, and 1100 aluminum to find that these materials exhibit the SDE, and demonstrated that the cause of the SDE is attributed to the fact that the flow stress of these materials is dependent on the hydrostatic pressure. Barlat et al. [2] conducted tension and compression tests on an aluminum alloy sheet (2090-T3) at increments of 15 degrees from the rolling direction (RD) to measure the respective 0.2% proof stresses, σ^T and σ^C. They found that σ^T was 12% larger than σ^C in the RD and that σ^C was several percent larger than σ^T in the directions 45°, 60°, 75°, and 90° from the RD, confirming the SDE. Kuwabara et al. [3] performed an in-plane compression test (IPCT) on a 5182-O aluminum alloy sheet and two low-carbon steel sheets using comb-shaped dies. They found that the flow stresses were higher in compression than in tension for the steel sheets, whereas the aluminum alloy sheet did not exhibit the SDE. Kuwabara et al. [4] concluded that the SDE in mild steel sheet is also due to the hydrostatic stress dependence

of flow stress. Holmen et al. [5] investigated the SDE of four 6000-series aluminum alloys (one was rolled and other three were extrude) in several tempers with yield strengths varying from 27 to 373 MPa. They observed that the axial stresses measured in compression tests were significantly higher than corresponding tensile stresses for nearly all material configurations. Ku et al. [6] experimentally verified the TCA in rolled aluminum alloy 7056 in the overaged condition (T7) with two tempers and reported that the TCA was attributed to the microstructural evolution. However, no experimental verification of the hydrostatic stress dependence of aluminum alloys has been reported, except for the work by Spitzig and Richmond [1].

This study investigates the SDE of a 6000-series rolled aluminum alloy sheet, A6116-T4, with a nominal thickness of 1.1 mm, which was age hardened for three months. In-plane tension and compression tests were performed to evaluate the SDE. Moreover, an equibiaxial tension test using a cruciform specimen [7] and a uniaxial compression test in the normal (through-thickness) direction (ND) of the test sample [4] were performed to clarify whether the flow stresses were affected by hydrostatic stress. It is found that the test sample exhibited the SDE and that the observed SDE can be attributed to the hydrostatic stress dependence of the yield stress.

Effect of hydrostatic stress on flow stress
Hereafter, the RD, transverse (TD), and ND of the material are referred to as the x-, y-, and z-axes, respectively. When the hydrostatic stress, $-\sigma_b$, is superimposed on the equibiaxial tensile stress state, σ_b, in the xy-plane, the equibiaxial tensile stress σ_b is cancelled by the hydrostatic stress $-\sigma_b$ and is equivalent to the uniaxial compressive stress state, $-\sigma_b$, in the z-axis (Fig. 1). Therefore, under the assumption that the flow stress of the material is independent of hydrostatic stress, the σ_b-$|\varepsilon_z^p|$ (ε_z^p: plastic strain in the z-axis direction) curve obtained from the equibiaxial tensile test should be identical to the $|\sigma_z^C|$-$|\varepsilon_z^p|$ curve obtained from the uniaxial compression test in the ND. On the other hand, if the flow stress is affected by hydrostatic stress, the two curves should be different from each other.
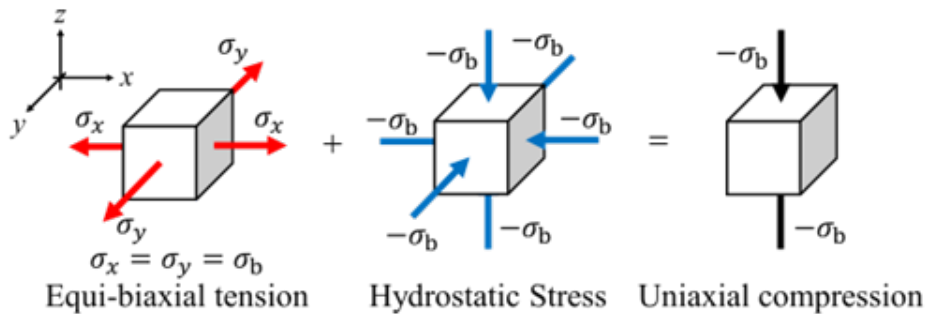

Fig. 1 Equivalence of the equibiaxial tension with the uniaxial compression with an assumption that the flow stress is independent of hydrostatic stress

Experimental method
Test material. The test sample was a 6000-series aluminum alloy sheet, A6116-T4, with a nominal thickness of 1.1 mm. It was 3-months age hardened. The mechanical properties of the sample are shown in Table 1.

Table 1 Mechanical properties of A6116-T4

Angle from RD [°]	Stress direction	E [GPa]	$\sigma_{0.2}$ [MPa]	r	σ_B [MPa]	ε_{TS}^p *	a** [MPa]	b** [MPa]	c**
0	Tension	69.5	142	0.707	251	0.199	323	195	11.7
	Compression	67.9	150	0.723					
90	Tension	67.7	137	0.671	244	0.209	319	195	11.0
	Compression	67.0	145	0.729					

* ε_{TS}^p is a logarithmic plastic strain giving the maximum tensile load
** Approximated using $\sigma = a - b\exp(-c\varepsilon^p)$ at $\varepsilon^p = 0.002 - \varepsilon_{TS}^p$

In-plane compression test. Fig. 2a and b show the IPCT apparatus used in this study. This apparatus was first developed in [3], modified in [8], and used in [9]-[11] for steel sheets. Fig. 2a shows an overview of the dies used for applying in-plane compression to a sheet specimen. Fig. 2b shows an overview of the test apparatus. Lower die 1 is bolted to the lower plate of the die set. Lower die 2 is bolted to the slide rail, so that the die can move in the horizontal direction without friction. A specimen is placed on lower dies 1 and 2 with both ends clamped by clamping jigs (not shown in the figure). Upper dies 1 and 2 are placed on the specimen. The positioning pins (not shown in the figure) fixed to upper dies 1 and 2 align with holes in lower dies 1 and 2. Accordingly, upper die 1 is stationary, and the motion of upper die 2 is synchronized with that of lower die 2. Lower die 2 is connected to a load cell to measure the tension-compression force during a test. It is actuated by hydraulic cylinder A to apply an in-plane tension-compression force to the specimen. Hydraulic cylinder B exerts a blank holding force on the specimen to prevent the buckling of the specimen during a test. The blank holding force is kept constant during a test via a hydraulic control valve. Steel cylindrical rollers are inserted between the blank holding platens and upper dies 1 and 2 so that the blank holding force can be transmitted to the specimen during an IPCT without friction. In this study, the blank holding force applied to the specimen was 1.2 % of 0.2 % yield stress (=1.7 MPa). The strain was measured using a strain gauge (YFLA-2-1LJC-F, Tokyo Measuring Instruments Laboratory Co. Ltd.). The strain rate was approximately 5×10^{-4} s^{-1} and the testing temperature was room temperature for both the tension and compression experiments.
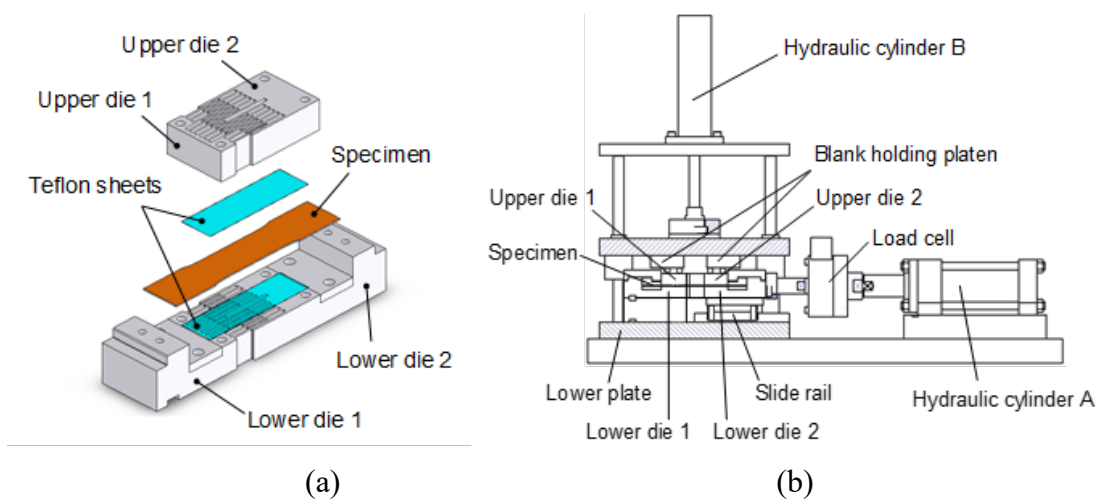

(a)   (b)

Fig. 2 IPCT devise [11]: (a) upper and lower dies and (b) overview of test apparatus

Uniaxial compression test of stacked specimen. Fig. 3a shows a schematic diagram of the uniaxial compression testing device for a stacked specimen. This device was incorporated into a regular tensile testing machine (AUTOGRAPH AG-100kNX, Shimadzu Corporation). Fig. 3b shows the details of a compression die. The compression dies have a thickness of 4 mm (a 3-mm-thick super steel base plate coated with 1-mm-thick sintered polycrystal diamond) and a diameter of 19 mm. Polycrystal diamond is effective for reducing the friction between the specimen and the compression dies and thus suppresses the non-uniform deformation of the specimen [12]. The compression dies were positioned on the upper and lower supporting plates using a clamping plate. The supporting plates were bolted to the upper and lower die plates. Since the initial thickness of the specimen was 1.1 mm, the amount of compressive displacement due to compression in the ND was small, making it difficult to measure plastic strain with high accuracy. Therefore, we stacked sheet samples in the ND and increased the initial thickness to 5.5 and 4.4 mm to improve measurement accuracy. The sheets were fixed with an adhesive (CEMEDINE Metal Lock Series Y610) to prevent interlaminar slippage.

Fig. 3c shows a schematic diagram of the uniaxial compression testing device for a stacked specimen. We performed compression tests using two stacked specimens with the same cross-sectional area but different heights, $h_H = 5.5$ mm and $h_L = 4.4$ mm, and measured the nominal stress-displacement for each specimen using a displacement meter (GT2-S5, KEYENCE Co. Ltd.). By denoting the difference in displacement between the two stacked specimens for a given nominal stress as Δu and calculating the compressive true strain, ε_z, as $\ln\left(1 - \frac{\Delta u}{h_H - h_L}\right)$, we determined the true stress-true strain curve, $\left|\sigma_z^C\right|$-$\left|\varepsilon_z\right|$, for a specimen with an initial stack height of $h\ (= h_H - h_L)$. This approach enabled us to exclude the influences of the elastic deformation of the compression
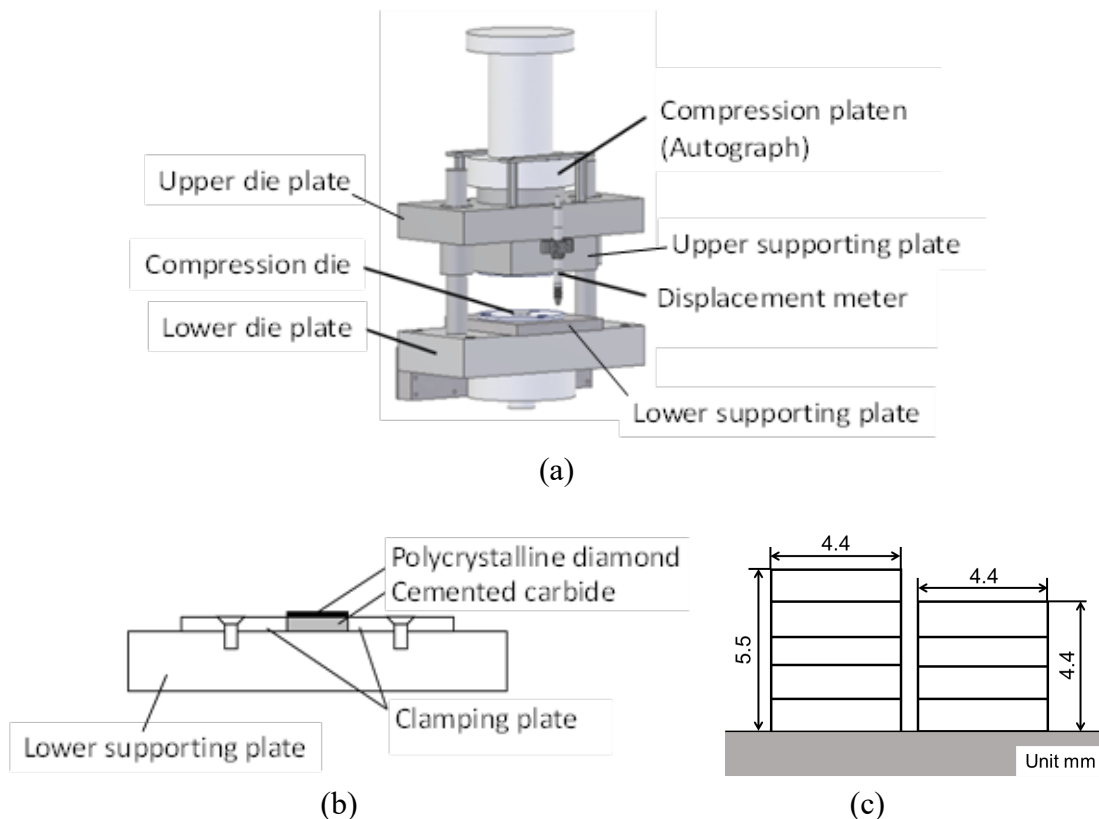

(a)

(b)

(c)

Fig. 3 SCT device [4]: (a) overview of test apparatus, (b) details of lower part of compression die, and (c) specimen geometry

device and potential friction between the specimen and compression plates on the measurement of $|\varepsilon_z|$. Thus, Young's modulus is calculated from the slope at unloading. We then determined the compressive true stress vs. compressive plastic strain curve, $|\sigma_z^C|$-$|\varepsilon_z^p|$.

Experimental results

Measurement of SDE. Fig. 4a and b compare the uniaxial tensile true stress-logarithmic plastic strain curves, $\sigma^T - \varepsilon^p$, with the compressive ones, $|\sigma^C|$-$|\varepsilon^p|$, for the RD and TD, respectively. Each curve is the average of two measurements. The compressive stress exceeds the tensile stress in both directions. Therefore, the SDE was clearly observed.

To quantitatively evaluate the magnitude of the SDE in the uniaxial stress state, the increase rate in the flow stress, $\beta_{\text{SDE}-\text{uni}}$, was defined as

$$\beta_{\text{SDE}-\text{uni}} = 2 \frac{|\sigma^C| - \sigma^T}{|\sigma^C| + \sigma^T} \tag{1}$$

where σ^T and $|\sigma^C|$ are the measured values at a given plastic work per unit volume, w^p. In the calculation of $\beta_{\text{SDE}-\text{uni}}$, both the uniaxial tension and in-plane compression test curves were averaged over two tests. Fig. 5 shows the variation of $\beta_{\text{SDE}-\text{uni}}$ with w^p for the RD and TD. It was found that $0.015 < \beta_{\text{SDE}-\text{uni}} < 0.053$ for the RD and $0.036 < \beta_{\text{SDE}-\text{uni}} < 0.066$ for the TD; therefore, the test sample clearly exhibited the SDE.

Verification of hydrostatic stress dependence of flow stress. Fig. 6 compares the σ_b-$|\varepsilon_z^p|$ curve measured using the equibiaxial tensile test with a cruciform specimen [1122], the average of two measurements, with the $|\sigma_z^C|$-$|\varepsilon_z^p|$ curve obtained from the uniaxial compression test in the ND of the stacked specimen. It can be clearly seen that the $|\sigma_z^C|$ exceeds the σ_b. Therefore, the flow stress of the test sample is affected by hydrostatic stress.

In order to quantitatively evaluate the effect of hydrostatic stress on flow stress, the plastic flow stress increase rate, $\beta_{\text{SDE}-\text{bs}}$, was defined as

$$\beta_{\text{SDE}-\text{bs}} = 2 \frac{|\sigma_z^C| - \sigma_b}{|\sigma_z^C| + \sigma_b} \tag{2}$$
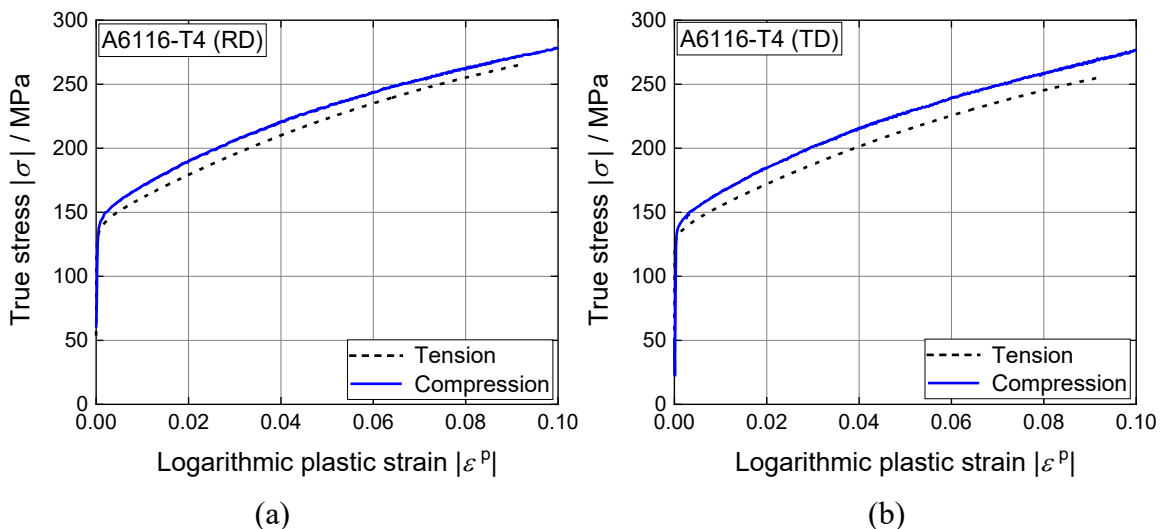

(a)   (b)

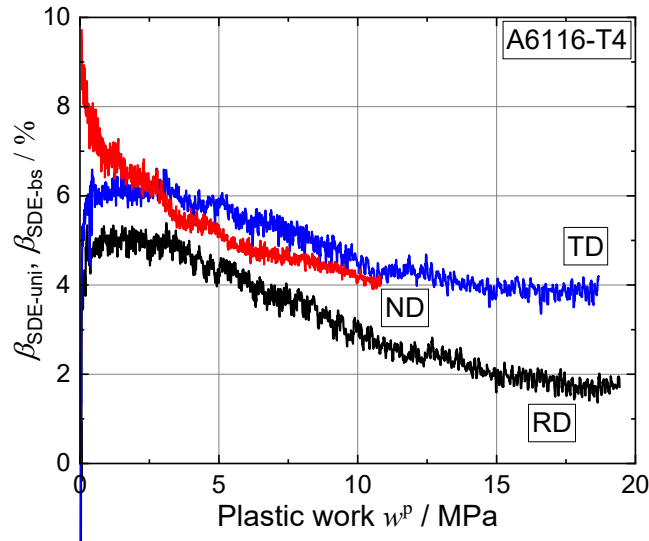*Fig. 4 Comparison of true stress-true strain curves between tension and compression in (a) RD and (b) TD*

Fig. 5 Change in $\boldsymbol{\beta_{SDE-uni}}$ and $\boldsymbol{\beta_{SDE-bs}}$ with plastic work per unit volume, $\boldsymbol{w^p}$
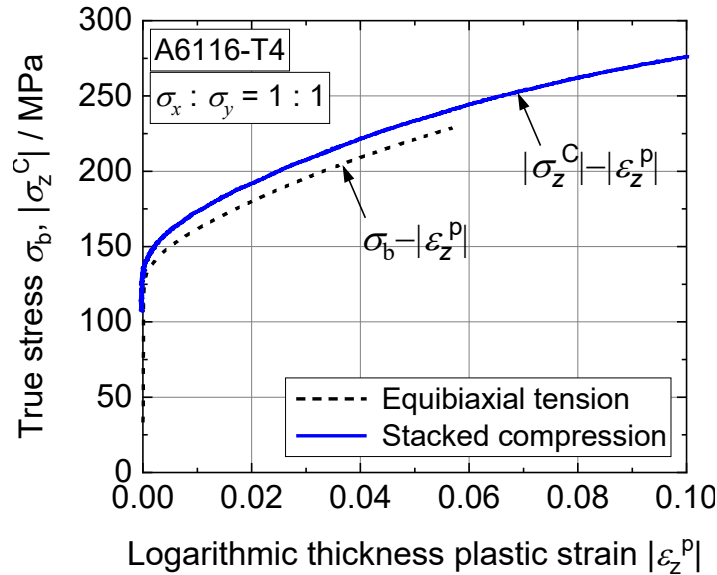
Fig. 6 Comparison of $\left|\boldsymbol{\sigma_z^C}\right|$-$\left|\boldsymbol{\varepsilon_z^p}\right|$ and $\boldsymbol{\sigma_b}$-$\left|\boldsymbol{\varepsilon_z^p}\right|$ curves

where σ_b and $\left|\sigma_z^C\right|$ are the measured values at a given plastic work per unit volume, w^p. The variation of β_{SDE-bs} with w^p is shown in Fig. 5. β_{SDE-bs} was in the range from 4 to 9 %. Therefore, we conclude that the flow stress of the test sample could be affected by hydrostatic stress.

Discussion
The Spitzig-Richmond yield condition [1] is given by

$$\bar{\sigma}(\boldsymbol{\sigma}) = c - \alpha c \operatorname{tr} \boldsymbol{\sigma} = c(1 - \alpha \operatorname{tr} \boldsymbol{\sigma}) \tag{3}$$

where $\boldsymbol{\sigma}$ is the stress tensor, $\operatorname{tr} \boldsymbol{\sigma}$ is its trace, $\bar{\sigma}$ is a pressure-independent effective stress, c is a strength parameter, and α is the pressure coefficient. Denoting the α measured using tension and

compression tests as α_{uni} and that measured using an equibiaxial tensile test and an SCT as α_{bs}, respectively, α_{uni} and α_{bs} are calculated as (see [4])

$$\alpha_{\mathrm{uni}} = \frac{|\sigma^{\mathrm{C}}| - \sigma^{\mathrm{T}}}{2|\sigma^{\mathrm{C}}|\sigma^{\mathrm{T}}} \tag{4}$$

$$\alpha_{\mathrm{bs}} = \frac{|\sigma_z^{\mathrm{C}}| - \sigma_{\mathrm{b}}}{3|\sigma_z^{\mathrm{C}}|\sigma_{\mathrm{b}}} \tag{5}$$

Considering that $\sigma^{\mathrm{C}} \approx \sigma_z^{\mathrm{C}}$ and $\sigma^{\mathrm{T}} \approx \sigma_{\mathrm{b}}$, we obtain the following equation:

$$\frac{\alpha_{\mathrm{bs}}}{\alpha_{\mathrm{uni}}} \approx \frac{|\sigma_z^{\mathrm{C}}| - \sigma_{\mathrm{b}}}{|\sigma^{\mathrm{C}}| - \sigma^{\mathrm{T}}} \times \frac{2}{3} \tag{6}$$

If α is a material constant, $\alpha_{\mathrm{bs}}/\alpha_{\mathrm{uni}}$ should be unity. It means that $(|\sigma_z^{\mathrm{C}}| - \sigma_{\mathrm{b}})/(|\sigma^{\mathrm{C}}| - \sigma^{\mathrm{T}})$ should be 3/2. However, from Fig. 5, it was measured that $(|\sigma_z^{\mathrm{C}}| - \sigma_{\mathrm{b}})/(|\sigma^{\mathrm{C}}| - \sigma^{\mathrm{T}}) \approx 1$ except for the early stage of plastic deformation, $w^{\mathrm{p}} < 0.2$ MPa. This suggests that there may be other influencing factors besides the hydrostatic pressure effect as a cause of the SDE in this material. Sun et al. [13] investigated the tension-compression (TC) asymmetry of a 6061 aluminum alloy using a strain gradient crystal plasticity model implemented with the finite element method. They concluded that the TC asymmetry for the aluminum alloys is caused by a combination of difference in the GND density and rotation of crystal matrix and particles, which is induced by plasticity even at the yield strain with limited plasticity. However, it is noted that they found that tensile flow stress was higher than compressive one. Therefore, the origin of the SDE in 6000-series aluminum alloys requires further study.

Conclusions

A uniaxial tensile test and an in-plane compression test were performed on a 6000-series aluminum alloy sheet (A6116-T4) to measure the SDE. In addition, an equibiaxial tensile test using a cruciform specimen and uniaxial compression tests in the ND using stacked specimens were performed to verify the hydrostatic stress dependence of the flow stress. The experimental findings obtained in this study are summarized follows.

(1) The SDE was observed for our test sample ($0.015 < \beta_{\mathrm{SDE-uni}} < 0.053$ for the RD and $0.036 < \beta_{\mathrm{SDE-uni}} < 0.066$ for the TD).

(2) The compressive stress, $|\sigma_z^{\mathrm{C}}|$, measured in the uniaxial compression test in the ND exceeded the equibiaxial tensile stress, σ_{b}, measured using a cruciform specimen. Therefore, the flow stress of the test sample could be affected by hydrostatic stress.

(3) There may be other influencing factors besides the hydrostatic pressure effect as a cause of the SDE in this material, as suggested by Sun et al. [13].

References

[1] W.A. Spitzig, O. Richmond, The effect of pressure on the flow stress of metals, Acta Metall 32 (1984) 457-463. https://doi.org/10.1016/0001-6160(84)90119-6

[2] F. Barlat, D.J. Lege, J.C. Brem, and C.J. Warren, Constitutive behavior for anisotropic materials and application to a 2090 Al-Li alloy, in: T.C. Lowe, A.D. Rollet, P.S. Follansbee and G.S. Daehn (Eds.), Modeling the Deformation of Crystalline Solids, The Minerals & Materials Society, 1991, pp. 189-203.

[3] T. Kuwabara, Y. Morita, Y. Miyashita, S. Takahashi, Elastic-Plastic Behavior of Sheet Metal Subjected to In-Plane Reverse Loading, in: Proc. Plasticity '95, The fifth international symposium

on plasticity and its current applications, ed. S Tanimura S, Khan AS, (1995) pp.841-844, Gordon and Breach Publishers.

[4] T. Kuwabara, R. Tachibana, Y. Takada, T. Koizumi, S. Coppieters, F. Barlat, Effect of hydrostatic stress on the strength differential effect in low-carbon steel sheet, Int. J. Material Forming 15 (2022) 13. https://doi.org/10.1007/s12289-022-01650-2

[5] J.K. Holmen, B.H. Frodal, O.S. Hopperstad, T. Børvik, Strength differential effect in age hardened aluminum alloys, Int. J. Plasticity 99 (2017) 144-161. https://doi.org/10.1016/j.ijplas.2017.09.004

[6] A.Y. Ku, A.S. Khan, T. Gnaupel-Herold, Quasi-static and dynamic response, and texture evolution of two overaged Al 7056 alloy plates in T761 and T721 tempers: Experiments and modeling, Int. J. Plasticity 130 (2020) 102679. https://doi.org/10.1016/j.ijplas.2020.102679

[7] ISO 16842:2021 Metallic materials −Sheet and strip – Biaxial tensile testing method using a cruciform test piece.

[8] T. Kuwabara, Y. Kumano, J. Ziegelheim, I. Kurosaki, Tension-compression asymmetry of phosphor bronze for electronic parts and its effect on bending behavior, Int. J. Plasticity 25 (2009) 1759-1776. https://doi.org/10.1016/j.ijplas.2009.01.004

[9] N. Noma, T. Kuwabara, Specimen Geometry Optimization for In-plane Reverse Loading Test of Sheet Metal and Experimental Validation, J. Jpn. Soc. Technol. Plast. 53 (617) (2012) 574-579.

[10] N. Noma, K. Hashimoto, T. Maeda, T. Kuwabara, Enhancement of Accuracy of Springback Simulation Using the Material Model Considering the Strength Differential Effect, J. JSTP 61(708) (2020) 20-25 (in Japanese).

[11] T. Maeda, N. Noma, T. Kuwabara, F. Barlat, Y.P. Korkolis, Measurement of the strength differential effect of DP980 steel sheet and experimental validation using pure bending test, J. Mater. Process. Technol. 256 (2018) 247-253. https://doi.org/10.1016/j.jmatprotec.2018.02.009

[12] T. Koizumi, M. Kuroda, Evaluation of tension-compression asymmetry of a low-carbon steel sheet using a modified classical compression test method, IOP Conf. Series, J. Phys. (2018) 1063. https://doi.org/10.1088/1742-6596/1063/1/012167

[13] F. Sun, S. Wang, Q. Xie, Role of particles and lattice rotation in tension-compression assymmetry of aluminium alloys, Int. J. Plasticity 159 (2022) 103464 https://doi.org/10.1016/j.ijplas.2022.103464